Study & comparative analysis of microstructure and mechanical properties of magnesium forged with cast components

Jay A Shah[1], PG Student, Department of Mechanical Engineering, MIT WPU, Maharashtra, India, shahj079@gmail.com

Shailendra P Shisode[2], Assistant Professor, Department of Mechanical Engineering, MIT WPU, Maharashtra, India, 1032200101@mitwpu.edu.in

Abstract - In automobile industry, there is always need for lightweight, higher efficiency and environmentally benefitted systems. With the need of futuristic material development, automobile applications are finding a way to replace existing material with Magnesium (Mg). In this study the main focus is on AZ91D alloy due to its most application in automotive and aerospace industries. Magnesium has 1.74 g/cm^3 density which is about one-third of aluminum, one quarter of steel and similar to polymers. Cast alloys are used in the majority of automotive magnesium applications. However, the trend is toward forged alloys, which rapidly expands the usage of forged magnesium, due to porosity and inclusion flaws in cast alloys. This paper presents analysis & structure property co-relation for commonly used AZ91 series alloys by their characterization to evaluate their interlinked properties. Results of mechanical properties and microstructural are correlated for AZ91 alloy systems for forged, cast and aged samples. The forged components showed improved mechanical properties overall when compared with the cast alloys. However, the issues of formability and high temperature behavior remain a source of concern. Understanding dominant deformation mechanisms and numerical modelling are critical for analyzing magnesium processing and manufacturing, as well as its behavior at high temperatures. The study aims to provide knowledge for correlating the microstructural and its mechanical properties by developing a constitutive model. Using the evolution of immobile dislocation density and excess vacancy concentration, a physically based constitutive model is created.

Keywords: AZ91D, Dislocation Model, Magnesium Forged, Mechanical Properties, Microstructural Characterization.

I INTRODUCTION

Magnesium (Mg) is observed as green material of modern era[1]. With the increasing fuel price range and the strict government norms, there is a need for lightweight applications for less fuel consumption and energy saving. Magnesium is also considered as a best choice of material in automobile, aerospace and electronic products[2][3]. Magnesium and its alloys have promising structural properties due to its low density, high strength-to-weight ratio, high specific strength, good thermal conductivity, better specific stiffness and excellent castability.

Daimler, Volkswagen Group, Ford and Jaguar are choosing Mg for structural components. Currently 14kg of magnesium is being used by VW Passat and Golf cars, which currently utilize AZ91D in drivetrain casings, offering about 20-25 % weight saving over aluminum[4][9][11]. Mg use to date has been limited to trimming and non-structural members for automobile applications. Increasing the load-bearing components with the use of Mg alloys with complex shapes requires a thorough understanding of Mg regarding its mechanical properties and microstructure right after the manufacturing process. Density of magnesium is 33% less than aluminum.

Magnesium-Aluminum alloys have a wider range of applications in industries[1][5]. In automotive industries, most magnesium alloys are produced by die-casting technique. Cast magnesium alloys, namely AZ91, have applications in powertrain, airbag supports, brake pedals, crankcase, steering wheel, etc. However, interior support structure of automobiles have die-cast AM50 and AM60 magnesium alloy. Die-casted magnesium alloys such as AM50 and AM60 are used for components which require better ductility. With limited ductility and strength of cast magnesium, there is a bend towards the usage of forged magnesium[6]. Forging process is usually employed to achieve better mechanical properties and proper

 DOI : 10.35291/2454-9150.2022.0393

homogenous microstructure. Wrought alloys have better properties than casting, but forging have better edge in cost competitiveness[7]. Wrought Mg alloys have refined grains and grain boundaries, better tensile properties, improved toughness which increases the opportunities for the use of Mg alloys as structural materials. Various studies shows that forged magnesium is best alternative to cast magnesium, aluminum, titanium and steel. Magnesium alloys have a problems like low hardness, poor plastic and corrosive properties compared to its peers. The primary purpose of using forged magnesium is the limited formability at lower temperatures due to small slip systems, active during deformation in the hexagonal close packaged (hcp) crystal structure ($c / a < \sqrt{3}$)[2]. Magnesium has only one slip system namely basal slip system $(0001)\langle 11\bar{2}0\rangle$ and the microstructure of Mg-Al forms a solid solution in its initial state and also $Mg_{17}Al_{12}$ phase.

II MATERIAL

Magnesium is the eighth most abundant element on the planet, is easily machined, and has the potential to be recyclable. The primary obstacle for magnesium alloys is its poor creep resistance at high temperatures above 120°C which makes its application limited. Most widely used alloying element is Aluminum which has low density and has strong strengthening effect on magnesium. Magnesium alloys are generally processed through casting due to higher mechanical anisotropy in forming process. Relationship between the mechanical properties and microstructure is required to predict the behavior of the magnesium alloy. Dini et. al.,[10] discovered and optimized the dislocation-based density model which provides the correlation between the internal parameters and its mechanical properties. Lindgren, Domkin and Hansson [13] found out the interdependence of the dislocations, dislocation density as well as the solid diffusion for the AISI 316L steel. These findings were then used for the wrought magnesium alloy for the development of the physical model.

III LITERATURE REVIEW

Many researches have studied about the magnesium alloy and its emerging usage in the automobile, aerospace industries. Lightweight application is the current research trend around the world. P.K. Mallik [8] discovered Mg as the best lightweight application. G.Cole and Sherman [4] studied the material characteristics for the Mg alloy and discovered the feasibility of Mg as lightweight application by studying the mechanical properties. Hong Tae and Terry Ostrom [7] predicts the behavior of forged and the cast components for its microstructure as well as mechanical properties. The various experiments were also conducted and the results were matched with the calibrated physical model to show the validity of model. Hoda Dinia et. al. [10] discovered and optimized the dislocation-based density model for the magnesium alloy considering various parameters. The model was optimized and calibrated for AZ91D. But it does not account for all the other internal state variables. Yangyang Guo et. al. [12] processed the microstructure and mechanical properties of AM80 magnesium alloy. Lindgren, Domkin and Hansson [13] found out the interdependence of the dislocations, dislocation density as well as the solid diffusion for the AISI 316L steel. These findings were then used for the wrought magnesium alloy for the development of the physical model. Limitations for this paper was that it didn't account for the process-parameters. Also, the model was valid upto a certain limit for a specific strain and strain rate values.

IV METHOD

A. Microstructure Test:

The die-cast AZ91D & AZ80A samples were selected for testing. The cast samples were solutionized at temperatures 420°C for 10 hours. For obtaining the microstructure and reveal its microstructural properties, polishing of the small cut samples of size 10 x 10 x 5 is required. Polishing is done using various grit papers namely 400,600,800,1250,2500 & 5000. Grit paper 400 is used to remove the dust particles, scratches and similarly grit paper 5000 is used for smooth finish. De-Mineralized (DM) water is used for polishing. For fine polishing, velvet cloth is used after using 5000 grit paper and silica mixture (2ml silica and rest DM water) is used as lubricant. To reveal the microstructures, etching is required to be done and it is achieved using nital (10% HNO_3 and rest ethanol). The testing is done in the Beuler Metaserve 250 polishing machine (Fig1). The RPM is set constant at 50.

Figure 1: Buehler Metaserv 250 Polishing Machine

B. Tensile Test:

Tensile test is done using Instron UTM machine as shown in Fig.2. A standard ASTM E8 dumbbell-shaped tensile specimen is selected for testing. Tensile test is done with loading of 0.40% strain value upto yield strength and 0.4mm/s strain value onwards with maximum load capacity of 50 kN. The test was conducted upto the failure point. These tests were conducted at room temperature. The cast as well as forged samples selected for testing. Along with the solutionized samples, the aged samples were also prepared at temperature 180°C for 24 hours. The typical AZ91 tensile test specimen is represented in Fig.3.

 DOI : 10.35291/2454-9150.2022.0393

Figure 2: Tensile Test Setup

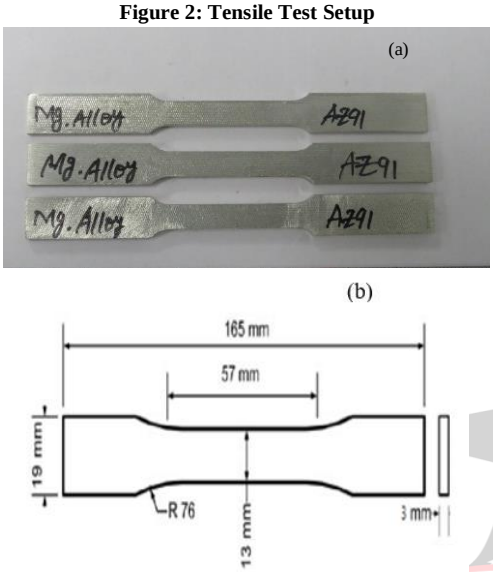

Figure 3: (a) Standard ASTM E8 AZ91 tensile specimen and (b) its dimensions

C. Hardness Test:

Hardness tests were conducted for both cast and forged specimens along the polished surface. The hardness was tested at the centre and its periphery of the polished surface. The cast samples were tested with the mold prepared with polished surface on top (Figure 4). The hardness was slightly decreased at centre for cast specimen. However, for specimens obtained from forging resulted with high values of hardness consistent throughout the thickness.

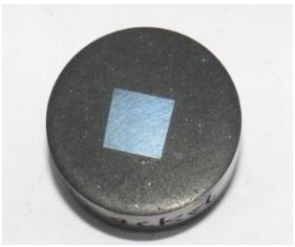

Figure 4: Polished sample within mold

V DEFORMATION MODEL

Flow stress consist of long-range barriers, σ_G, which is independent of temperature and a component of short-range barriers, σ^*, which are temperature dependent. Flow stress is given by sum of component which resist motion of dislocation as follows[14][15][16]:

$$\sigma_y = \sigma_G + \sigma^* \quad (1)$$

Long range dislocations are because of immobile dislocations in substructures, given as[14]

$$\sigma_G = m\alpha Gb\sqrt{\rho_i} \quad (2)$$

where m is Taylor orientation factor, α is proportionality factor and ρ_i is immobile dislocations.

σ^* is the stress to surpass short-range obstacles and move across the lattice. A moving dislocation waits in front of an obstacle and this time is waiting time. Boltzmann law of energy distribution defines this frequency related to probability, that dislocation energy must exceeds the required activation energy to surpass obstacles. Average velocity to pass obstacle depends on Gibbs free energy ΔG and temperature T [17], defined as:

$$\bar{v} = \Lambda \upsilon_a \exp\left(-\frac{\Delta G}{kT}\right) \quad (3)$$

where Λ is the mean free path, υ_a is the frequency of attempt and k is the Boltzmann constant. Orowan's equation defines plastic strain in terms of dislocation density and velocity[18], as follows:

$$\dot{\varepsilon}^p = \frac{\rho_m b \bar{v}}{m} \quad (4)$$

where $\bar{v}$ is the mean velocity of mobile dislocations with a density of ρ_m. Further, eq.4 reconstructed as:

$$\dot{\varepsilon}^p = \frac{\rho_m \Lambda b \upsilon_a}{m} exp\left(-\frac{\Delta G}{kT}\right) \quad (5)$$

The dislocation motion is totally assisted by thermal energy. The probability that the dislocation surpasses the obstacle increase with the increase in the temperature if the stress is not sufficient to pass a dislocation over the barrier with activation energy, ΔG. A generalized equation for the shape of barrier is given by two parameters – p & q [19]:

$$\Delta G = \Delta F\left[1 - \left(\frac{\sigma^*}{\sigma_{ath}}\right)^p\right]^q \quad (6)$$

Here, ΔF is the total free energy required for a dislocation to overcome the lattice resistance or obstacles[17], σ_{ath} is the athermal flow strength required to move dislocations across lattice. The exponents $0 < p \leq 1$ and $0 < q \leq 2$ are linked with the shape of energy barriers. The pre-exponential term in Eq.5 is expressed as [17]:

$$\dot{\varepsilon}_{ref} = \frac{\rho_m \Lambda b \upsilon_a}{m} \quad (7)$$

where $\dot{\varepsilon}_{ref}$ is the reference strain rate. Combining Eqs. (5), (6), and (7):

$$\dot{\varepsilon}^p = \dot{\varepsilon}_{ref}\, exp\left\{-\frac{\Delta F}{kT}\left[1 - \left(\frac{\sigma^*}{\sigma_{ath}}\right)^p\right]^q\right\} \quad (8)$$

Here, $\Delta F = \Delta f_0 G b^3$ is activation energy required to surpass lattice resistance in the absence of any external force, and $\sigma_{ath} = \tau_0 G$ is shear strength in the absence of thermal energy. Table 1 represents the factors Δf_0 and τ_0. Here L represents the mean spacing of the obstacles, precipitates or solutes[17].

 DOI : 10.35291/2454-9150.2022.0393

Table 1: Activation energy factor and shear strength of different obstacles

Obstacle Strength	Δf_o	τ_0	Example
Strong	2	$> \frac{b}{L}$	Strong precipitates
Medium	0.2-1.0	$\approx \frac{b}{L}$	Weak precipitates
Weak	<0.2	$\ll \frac{b}{L}$	Lattice Resistance

The short-range dislocations can be derived from Eq. (1) as a function of effective plastic strain as [19][20][21]:

$$\sigma^* = \tau_0 \, G \left\{ 1 - \left[\frac{kT}{\Delta f_0 G b^3} \ln \left(\frac{\dot{\varepsilon}_{ref}}{\dot{\varepsilon}_p} \right) \right]^{\frac{1}{q}} \right\}^{\frac{1}{p}} \quad (9)$$

Evolution of Immobile Dislocation Density

$$\dot{\rho}_i = \dot{\rho}_i^{(+)} + \dot{\rho}_i^{(-)} \quad (10)$$

Mobile dislocations become immobilised or annihilated when they move over mean free path Λ. On the other hand, immobile dislocation density is assumed to increase proportionally to plastic strain rate, which is inversely proportional to mean free path and directly to mobile dislocation density [22][23]:

$$\dot{\rho}_i^{(+)} = \frac{m}{b} \frac{1}{\Lambda} \dot{\varepsilon}_p \quad (11)$$

where m is the Taylor orientation factor. The mean free path can be given as

$$\frac{1}{\Lambda} = \frac{1}{\lambda_2} + \frac{1}{s} \quad (12)$$

where λ_2 is SDAS and s is subgrain or subcell diameter. Immobile dislocation density plays an important role in formation and evolution of subcells related to factor Kc

$$s = K_c \frac{1}{\sqrt{\rho_i}} \quad (13)$$

Recovery processes

Recovery of dislocation densities can be done by different processes. Recovery or remobilization process is corelated with current dislocation density which is governed by dislocation climb and glide. Recovery of dislocation glide is given by [17][24]

$$\dot{\rho}_{i,glide}^{(-)} = \Omega \dot{\rho}_i \dot{\varepsilon}^p \quad (14)$$

where Ω is temperature dependent recovery function. Dislocation climb is assumed to be [25]:

$$\dot{\rho}_{i,climb}^{(-)} = 2 C_\gamma D v \frac{C_v}{C_v^{eq}} \frac{G b^3}{kT} \left(\rho_i^2 - \rho_{eq}^2 \right) \quad (15)$$

where c_v is current vacancy concentration and c_v^{eq} is equilibrium vacancy concentration. The dislocation density reduces towards an equilibrium value of ρ_{eq}.

VI Results

A. Tensile Test:

The aim of study was to compare the mechanical properties and microstructure characteristics of cast as well as forged specimens. This included the comparison of the yield stress, elongation (in %) and the UTS (Ultimate Tensile Strength) value. The comparison between these three properties is depicted in Fig.6. For each type at least 8 samples of grade AZ91D and AZ80A were tested. The aged samples, kept at temperature 180°C for 24 hours, were also considered. The results of yield stress for solutionized sample and aged samples were almost equal but much greater than cast sample. The UTS value were also similar for solutionized as well as aged sample which is quite appreciable value than the as cast component. And elongation for solutionized material was highest in comparison of both samples. The results showed the improved properties of forged components of AZ91D & AZ80A than cast components. The reasons may include porosity and precipitates formed during the casting process. The true stress v/s strain is plotted for cast, forged as well as for aged sample (Fig.5). It was depicted that the yield point for aged sample is highest which shows more elastic region of the component. The failure point of cast material is very low which means that that it cannot sustain under high loads. Whereas for forged material it has high UTS. The strain value for forged sample is maximum. This implies that the ductility of that material has been improved.

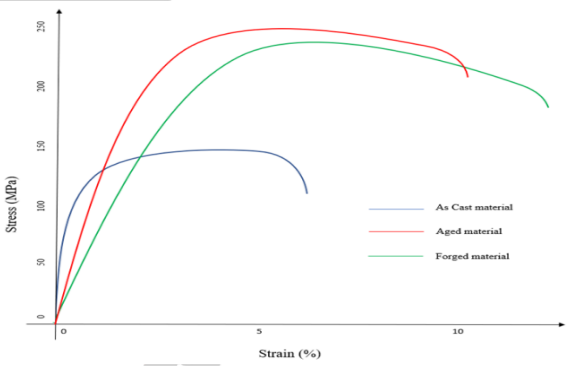

Figure 5: Stress Strain curves for various specimens

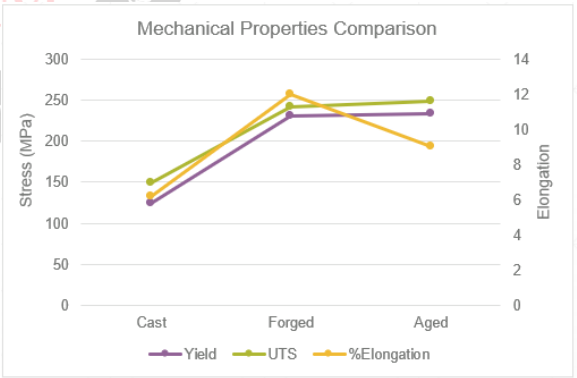

Figure 6: Comparison of Mechanical Properties

B. Microstructure:

The microstructure of the specimens of die-cast and forged magnesium alloys were observed at 761X and 500X magnification to determine the behavior of different phases. The intermetallic phases are visible in the microstructure which shows $Mg_{17}Al_{12}$ and Al_8Mn_5 (refer Fig.7(a),(b),(c),(d)). Under non–equilibrium solidification conditions, the microstructure of AZ91 alloy has a dendritic form in which brittle β– $Mg_{17}Al_{12}$ phase exists between

 DOI : 10.35291/2454-9150.2022.0393

dendrite arms. The intermetallic phases present decreases the overall strength of structure. The black structure represents pure primary α-Mg. A number of porosities observed in cross section of specimen in the as-cast specimen. The SDAS (Secondary Dendrite Arm Spacing) were observed more in cast specimens than forged specimen. The forged specimen on the other hand revealed better grain boundaries and grains. As seen a number of undissolved phases are revealed in the microstructure. SDAS decreases the hardness, tensile strength and percent elongation for a specimen.

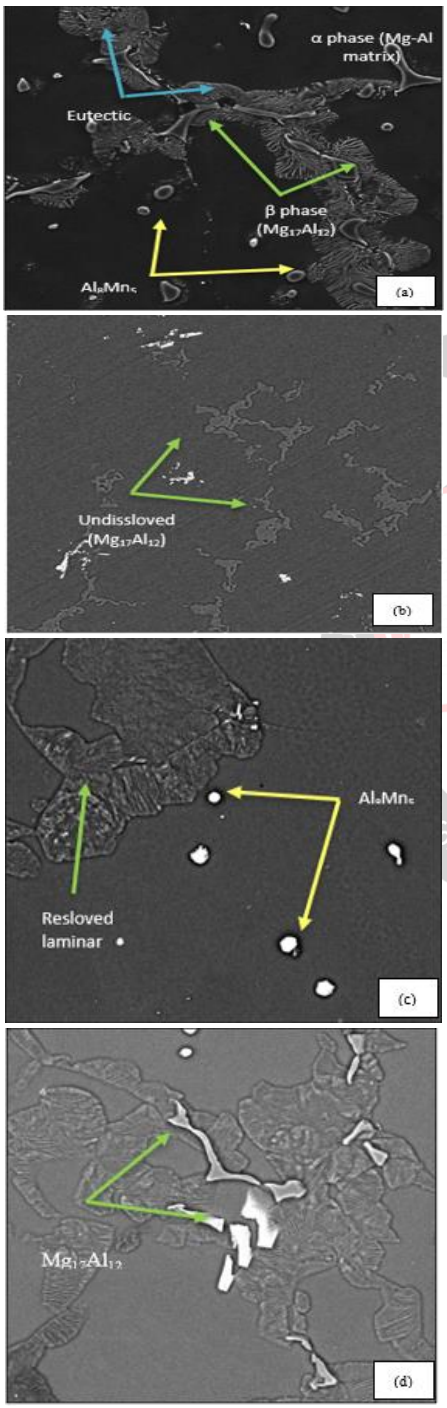

Figure 7: (a), (b) Microstructure of AZ91D in cast and forged state; (c), (d) Microstructure of AZ80A in cast and forged state

C. Hardness Test:

Hardness test was done on three samples namely – Aged sample quenched in MgO powder, AZ91 forged sample and AZ80 cast sample. Vickers Hardness test was conducted with 5 kgf test load. Table 2 represents the hardness values at different locations in polished surface. The forged component has greater hardness value due to the heat treatment process. The fine grains achieved during this process increases the resistance to dislocation movement resulting in strain hardening of the material.

Table 2: Hardness Values

Sr. No	Component Name	Hardness Value	Average Hardness Value
1	Aged (Quenched in MgO powder) Sample	62.5 62.1 68	64.2
2	Forged Sample	54.7 56.1 56.7	55.83
3	Cast Sample	86.4 90.2 78.4	85.0

VII CONCLUSIONS

This study presents the tensile, microstructure and hardness properties of cast and forged magnesium alloy AZ91D and AZ80A. From these studies, the specimens produced showed different tensile strength, hardness and microstructure. Cast components showed poor tensile strength, lower hardness value as compared to the forged components, due to porosity and microstructural inhomogeneities. The ultimate strength, along with ductility, observed for forged was much higher than that of cast sample which shows its applications in crash or high strength requirements. The stain values for forged components showed improved characteristics than cast which fits its application with the requirement of high elongation of material. Die cast microstructure of AZ91 consisted α-Mg and intermetallic phase $Mg_{17}Al_{12}$. The microstructure of forged magnesium alloy had better grains with refined grain boundaries and less impurities. The hardness value was less at the center than those at the surface.

VIII ACKNOWLEDGMENT

The authors gratefully acknowledge the financial support of this work by Automotive Research Association of India.

IX REFERENCES

[1] Yan Yang, Xiaoming Xiong, Jing Chen, Xiaodong Peng, Daolun Chen, Fusheng Pan; Research advances in magnesium and magnesium alloys worldwide in 2020.

[2] J. Hirsch, Aluminium in innovative light-weight car design, Materials Transactions 52(5) (2011) 818-824.

 DOI : 10.35291/2454-9150.2022.0393

[3] M.K. Kulekci, Magnesium and its alloys applications in automotive industry, The International Journal of Advanced Manufacturing Technology 39(9) (2008) 851-865.

[4] G. Cole, A. Sherman, Lightweight materials for automotive applications, Materials characterization 35(1) (1995) 3-9.

[5] A.A. Luo, Magnesium casting technology for structural applications, Journal of Magnesium and Alloys 1(1) (2013) 2-22.

[6] I. Polmear, Magnesium alloys and applications, Materials science and technology 10(1) (1994) 1-16.

[7] Hong Tae Kang, Terry Ostrom; Mechanical behavior of cast and forged magnesium alloys and their microstructures.

[8] P.K. Mallick, Materials, design and manufacturing for lightweight vehicles, Elsevier2010.

[9] A. Stalmann, W. Sebastian, H. Friedrich, S. Schumann, K. Dröder, Properties and processing of magnesium wrought products for automotive applications, Advanced Engineering Materials 3(12) (2001) 969-974.

[10] Hoda Dinia, Ales Svobodab, Nils-Eric Anderssona, Ehsan Ghassemalia, Lars-Erik Lindgrenb, Anders E.W. Jarforsa; Optimization and validation of a dislocation density based constitutive model for as-cast Mg-9%Al-1%Zn

[11] A.A. Luo, Magnesium: current and potential automotive applications, Jom 54(2) (2002) 42-48.

[12] Yangyang Guo, Houhong Pan, Lingbao Ren, Gaofeng Quan; Microstructure and mechanical properties of wire arc additively manufactured AZ80M magnesium alloy.

[13] Lars-Erik Lindgren, Konstantin Domkin, Sofia Hansson; Dislocations, vacancies and solute diffusion in physical based plasticity model for AISI 316L.

[14] A. Seeger, The mechanism of glide and work-hardening in FCC and HCP metals, Dislocation and mechanical properties of crystals (Fischer, JC, Johnston, WG, Thomson, R., eds.) (1956) 243.

[15] Y. Bergstrom, Dislocation model for the stress-strain behaviour of polycrystalline alpha-iron with special emphasis on the variation of the densities of mobile and immobile dislocations, MAT SCI ENG 5(4) (1970) 193-200.

[16] U. Kocks, Laws for work-hardening and low-temperature creep, ASME, Transactions, Series H-Journal of Engineering Materials and Technology 98 (1976) 76-85.

[17] H.J. Frost, M.F. Ashby, Deformation mechanism maps: the plasticity and creep of metals and ceramics, (1982).

[18] E. Orowan, Symposium on Internal Stresses in Metals and Alloys, Institute of Metals, London 451 (1948).

[19] U. Kocks, A. Argon, M. Ashby, In Chalmers, B., Christian, JW and Massalski, TB (Eds.) Thermodynamics and Kinetics of Slip (Progress in Materials Science, Vol. 19), Pergamon, Oxford, 1975.

[20] H. Mecking, U. Kocks, Kinetics of flow and strain-hardening, Acta Metallurgica 29(11) (1981) 1865-1875.

[21] S. Nemat-Nasser, W.-G. Guo, D.P. Kihl, Thermomechanical response of AL-6XN stainless steel over a wide range of strain rates and temperatures, Journal of the Mechanics and Physics of Solids 49(8) (2001) 1823-1846.

[22] Y. Bergström, H. Hallen, Hall–Petch relationships of iron and steel, Metal science 17(7) (1983) 341-347.

[23] Y. Estrin, A. Finel, M. Veron, D. Mazière, Thermodynamics, microstructures, and plasticity, NATO advanced study institute on thermodynamics. Microstructures and plasticity, Kluwer Academic Publishers, France (2002) 217-238.

[24] Y. Bergitrom, The Plastic Deformation of Metals-a Dislocation Model and Its Applicability, Rev. Powder Metall. Phys. Ceram. 2(2) (1983) 79-265.

[25] J. Friedel, International Series of Monographs on Solid State Physics. Vol. 3: Dislocations, Pergamon Press, 0xford, England, 1964.

 DOI : 10.35291/2454-9150.2022.0393